Advanced Robotics, Vol. 20, No. 9, pp. 1015–1034 (2006)

Also available online - www.vsppub.com

Full paper

Development of hybrid hydraulic–electric power units for field and service robots

KURT AMUNDSON, JUSTIN RAADE, NATHAN HARDING and H. KAZEROONI *

Department of Mechanical Engineering, University of California, Berkeley, CA 94720, USA

Received 13 September 2005; accepted 27 March 2006

Abstract—Energetic autonomy of a hydraulic-based mobile robot requires a power source capable of both hydraulic and electrical power generation. The hydraulic power is used for locomotion, and the electric power is used for the control computer, sensors and other peripherals. In addition, the power source must be lightweight and quiet. This study presents several designs of internal combustion engine-based power units. Each power unit is evaluated with a Ragone plot which shows its performance over a wide range of operation times. Several hydraulic–electric power units (HEPUs) were built and successfully demonstrated on the Berkeley lower extremity exoskeleton (BLEEX). The best-performing design of the HEPUs, based upon the Ragone plot analysis, is described in detail. This HEPU produces constant pressure hydraulic power and constant voltage electric power. The pressure and voltage are controlled on board the power unit by a computer. A novel characteristic of this power unit is its cooling system in which hydraulic fluid is used to cool the engine cylinders. The prototype power unit weighs 27 kg and produces 2.3 kW (3.0 hp) hydraulic power at 6.9 MPa (1000 p.s.i.) and 220 W of electric power at 15 V DC.

Keywords: Mobile power sources; hydraulic power; field and service robots; exoskeletons; BLEEX.

1. INTRODUCTION

Most human-scale and field robotic systems are currently powered by tethers or heavy battery systems. In order for a robotic device to obtain energetic autonomy free from tethers and heavy batteries, a compact, portable power unit providing both mechanical power for actuation and electrical power for computation and control is essential. The NiMH battery pack in ASIMO, Honda's humanoid walking robot, is one example of a battery-based power unit [1]. However, batteries have a low specific energy (energy per unit mass): 0.54 MJ/kg for a high-performance lithium

*To whom correspondence should be addressed. E-mail: kazerooni@berkeley.edu

ion battery [2]. Due to this low specific energy, batteries become large and heavy unless the operation time is short or the robotic system requires little power.

A fuel with a higher specific energy than batteries is desirable in a mobile robotic system. Previous work at UC Berkeley focused on the use of a monopropellant-powered free piston hydraulic pump [3, 4]. This system generates hydraulic power through decomposition of 90% concentrated hydrogen peroxide. Monopropellants are more energetic than batteries, but their specific energy (1.2 MJ/kg for 90% concentrated hydrogen peroxide) is significantly lower than that of a fuel such as gasoline (44 MJ/kg). Simplicity is a key advantage of monopropellants. The system requires no premixing, air compression, ignition or cooling system. All one needs is to control the amount of monopropellant fuel through a solenoid valve. However, the relatively low specific energy, the substantial required safety features and the fuel cost prevented us from further pursuing monopropellant-based power units for robotic applications. See Refs [5, 6] for another novel utilization of monopropellant in which fuel is directly converted to mechanical power.

Internal combustion (IC) engines utilize the high specific energy of gasoline. The power units described here utilize IC engines to produce compact, lightweight power sources. This is primarily motivated by the fact that IC engines have been the primary source of power for automobiles, earthmoving machinery, motorcycles, and other wheeled vehicles. We envision mobile field robots as another class of these field vehicles that operate outdoors for periods of hours. In fact, several field and service robotic systems have already experimented with IC engines as their prime mover [7, 8].

This paper describes the basic design challenges in general for an IC engine-based hydraulic–electric power unit (HEPU) for robotic applications (see also Refs [9, 10]). First, an analysis of the HEPU systems based on Ragone plots is presented. Then, the specifications of several versions of the HEPU are described. Lastly, the completed architecture of the final HEPU, including its hydraulic and electric power generation, cooling system, and control, is described in detail.

2. RAGONE PLOT ANALYSIS

Ragone plots are useful for evaluating the performance of a power unit for a wide range of operation times [11]. They plot the power unit's specific power (power divided by total mass) versus the specific energy (energy divided by total mass). The specific energy $\hat{E}$ can be expressed by:

$$\hat{E} = \frac{E_{\text{tot}}}{m_{\text{tot}}} = \frac{P_{\text{tot}}\tau}{m_{\text{fuel}} + m_{\text{tank}} + m_{\text{eng}}}, \tag{1}$$

where E_{tot} is the total energy required for the operation time τ of the system, m_{tot} is the total power unit mass including the mass of the fuel m_{fuel}, fuel tank m_{tank} and engine m_{eng}, and P_{tot} is the total output power (hydraulic power plus electrical

power). The mass of the fuel is:

$$m_{\text{fuel}} = \frac{E_{\text{tot}}}{\eta \hat{h}}, \tag{2}$$

where $\hat{h}$ is the specific energy of the fuel and η is the overall efficiency. The overall efficiency is defined as the total output power divided by the fuel power (measured fuel flow rate $\dot{m}_{\text{fuel}}$ times specific energy $\hat{h}$ of the fuel) flowing into the engine:

$$\eta = \frac{P_{\text{tot}}}{\dot{m}_{\text{fuel}} \hat{h}}. \tag{3}$$

The mass of the fuel tank is proportional to the mass of the fuel, and can be expressed by:

$$m_{\text{tank}} = \frac{m_{\text{fuel}}}{\beta}, \tag{4}$$

where β is a constant defined as the ratio of fuel mass to the mass of the tank required to hold the fuel. Using (2) and (4) in (1) and simplifying produces:

$$\hat{E} = \left[\frac{1}{\eta \hat{h}} \left(1 + \frac{1}{\beta} \right) + \frac{m_{\text{eng}}}{P_{\text{tot}} \tau} \right]^{-1}. \tag{5}$$

The specific power $\hat{P}$ can be similarly expressed as:

$$\hat{P} = \frac{P_{\text{tot}}}{m_{\text{tot}}} = \frac{\hat{E}}{\tau}. \tag{6}$$

Several valuable trends can be learned by examining a Ragone plot. As the operation time τ becomes very long, the specific power $\hat{P}$ approaches zero while the specific energy $\hat{E}$ tends toward a finite value. This can be shown by examining (5) and (6) as the operation time approaches infinity:

$$\begin{aligned} &\lim_{\tau \to \infty} \hat{E} = \eta \hat{h} \left(\frac{\beta}{\beta + 1} \right), \\ &\lim_{\tau \to \infty} \hat{P} = 0. \end{aligned} \tag{7}$$

Alternatively, as the operation time becomes very short, the specific energy approaches zero while the specific power approaches a finite value. As the operation time approaches zero, (5) and (6) become:

$$\begin{aligned} &\lim_{\tau \to 0} \hat{E} = 0, \\ &\lim_{\tau \to 0} \hat{P} = \frac{P_{\text{tot}}}{m_{\text{eng}}}. \end{aligned} \tag{8}$$

If one is concerned with very long operation times for a mobile robotic power unit, then (7) shows that the most critical parameters of the power unit are the overall

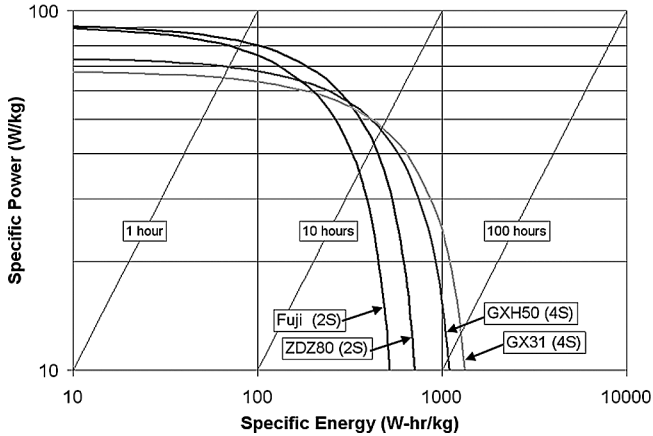

Figure 1. Ragone plot of HEPU systems, labeled by engine name. The two-stroke power units are labeled '2S' and the four-stroke power units are labeled '4S'.

efficiency, the specific energy of the fuel and the fuel storage ratio. For a power unit designed for very short operation times, (8) shows that the most critical parameters are the total power and the engine mass (the fuel and fuel tank mass are negligible).

Mobile robotics require lightweight power units in order to operate effectively in the field. Therefore, it is imperative to find the lightest power unit for a given operation time. Using a Ragone plot to evaluate the power units described in this work enabled us to determine the lightest choice for a given application. Figure 1 shows a Ragone plot of each HEPU system developed at the UC Berkeley. All the HEPU systems use gasoline with a fuel storage ratio $\beta = 4$ (based on a sturdy plastic tank holding the gasoline). The diagonal lines correspond to constant operation times on a logarithmic scale. Based on the information illustrated in Fig. 1, for operation times less than approximately 10 h the lightest power unit is the ZDZ80-based HEPU due to its high specific power. For very long operation times, longer than 10 h, the lightest system is the GX31-based HEPU due to its high overall efficiency. In general, two-stroke engines have a higher specific power than four-stroke engines, making the two-stroke HEPU systems lighter for short operation times. Four-stroke engines, on the other hand, have a higher efficiency than two-strokes, making the four-stroke HEPU systems lighter for long operation times.

3. SEQUENCE OF HEPU DESIGNS

3.1. General architecture

All of the HEPU designs presented in this work have the same general architecture as shown in Fig. 2. The engine provides the shaft power which turns a hydraulic pump to produce hydraulic flow for the actuators of the robotic system. The engine also spins an alternator which provides electrical power for the sensors, control

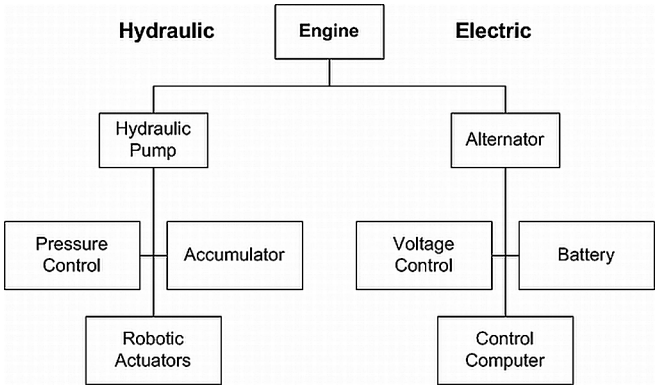

Figure 2. HEPU system architecture.

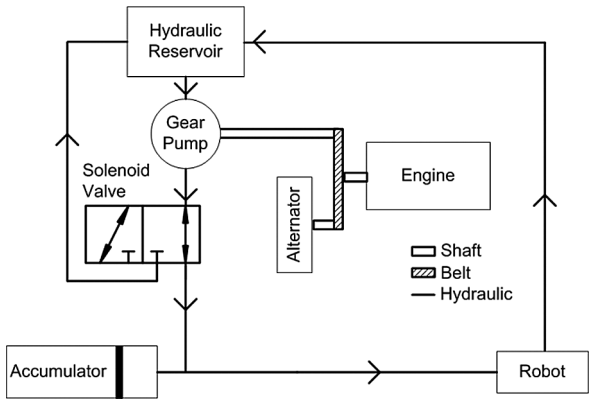

Figure 3. Hydraulic schematic of the GX31 HEPU.

computers and ancillary equipment such as cooling fans or pumps. The power units described herein can be utilized by any hydraulic robotic system.

3.2. Honda GX31-based HEPU

The Honda four-stroke engine GX31 serves as the prime mover in the first-generation HEPU. A hydraulic schematic for the GX31-based HEPU is shown in Fig. 3.

The engine spins a gear pump and alternator *via* a belt drive. A solenoid valve maintains the hydraulic pressure by rerouting the flow from the pump back to the reservoir when the pressure in the accumulator reaches the desired value. An independent speed governor on the engine maintains the electrical voltage by maintaining a constant engine speed. A photograph of the system is shown in Fig. 4. The system specifications are listed in Table 1. The GX31 HEPU proved to be a lightweight power unit suitable for a robotic system with low hydraulic flow requirements.

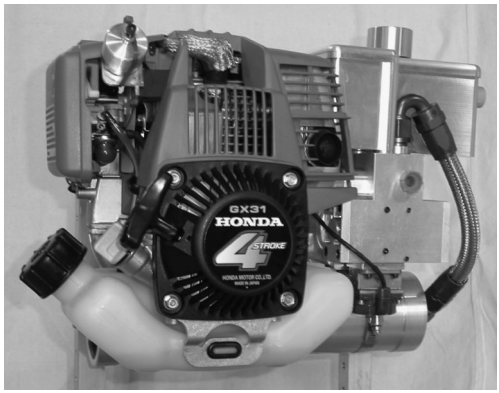

Figure 4. Honda GX31 HEPU.

Table 1.
GX31 HEPU specifications

Description	First-generation HEPU
Engine	Honda GX31 4-stroke, air-cooled, centrifugal clutch
Hydraulic power	750 W (5.3 LPM @ 6.2 MPa)
	1.0 HP (1.4 GPM @ 900 p.s.i.)
Electrical power	120 W (Aveox three-phase brushless motor/alternator)
Transmission	Double belt drive with hydraulic pump and electrical alternator
Hydraulic pump	Haldex W600 gear pump
Pressure and voltage control	Solenoid hydraulic bypass valve, bang-bang throttle control
Overall efficiency (η)	16%
Mass without fuel or tank (m_{eng})	13 kg (28 lb)

3.3. Honda GXH50-based HEPU

The second-generation HEPU has the same hydraulic and electrical architecture as the first-generation HEPU (Fig. 3), but utilizes the Honda four-stroke engine GXH50 for a significant power increase over the GX31. This power unit was used extensively for field testing of the Berkeley lower extremity exoskeleton (BLEEX) [12–14]. Figure 5 shows a photograph of the system. The system specifications are listed in Table 2.

3.4. Fuji BT50SA-based HEPU

A two-stroke engine (the Fuji BT50SA) was chosen for a new HEPU design due to its light weight and high power output [15]. Figure 6 shows a hydraulic schematic of the Fuji-based HEPU. In contrast to the previous HEPU systems, an electrically actuated clutch maintains hydraulic pressure by disconnecting the engine from the pump when the desired pressure is reached in the accumulator. A computer-aided design (CAD) image of the system is shown in Fig. 7. The system specifications are

Figure 5. Honda GXH50 HEPU.

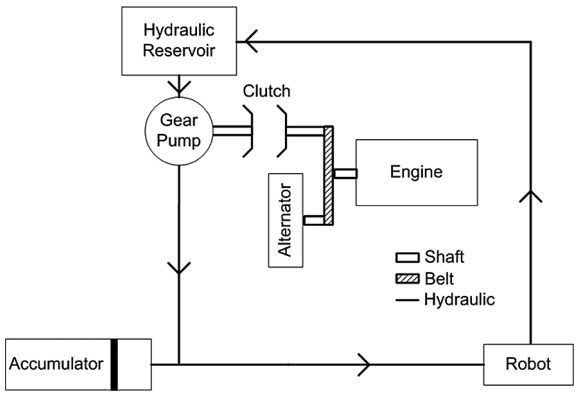

Figure 6. Hydraulic schematic of the Fuji BT50SA HEPU.

Table 2.
GXH50 HEPU specifications

Description	Second-generation HEPU
Engine	Honda GXH50 4-stroke, air-cooled, centrifugal clutch
Hydraulic power	1.0 kW (9.1 LPM @ 6.9 MPa) 1.4 HP (2.4 GPM @ 1000 p.s.i.)
Electrical power	100 W (Faulhaber three-phase brushless motor/alternator)
Transmission	Double belt drive with hydraulic pump and electrical alternator
Hydraulic pump	Haldex W600 gear pump
Pressure and voltage control	Solenoid hydraulic bypass valve, stock governor throttle control
Overall efficiency (η)	13%
Mass without fuel or tank (m_{eng})	15 kg (34 lb)

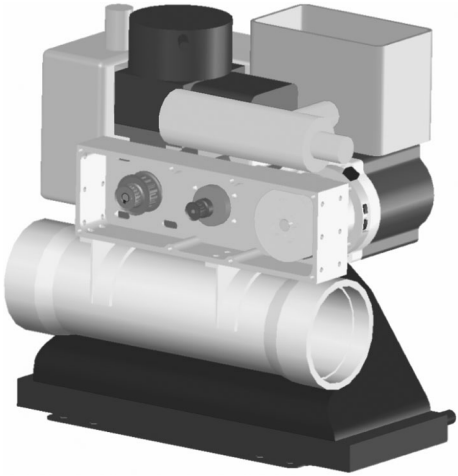

Figure 7. CAD model of the Fuji BT50SA HEPU.

Table 3.
Fuji BT50SA HEPU specifications

Description	Third-generation HEPU
Engine	Fuji BT50SA 2-stroke, liquid-cooled, solenoid-activated clutch
Hydraulic power	1.1 kW (15 LPM @ 4.1 MPa) 1.5 HP (4.0 GPM @ 600 p.s.i.)
Electrical power	120 W (Aveox three-phase brushless motor/alternator)
Transmission	Double belt drive with hydraulic pump and electrical alternator
Hydraulic pump	Haldex W600 gear pump
Pressure and voltage control	Bang-bang electric clutch bypass, computer-controlled engine speed
Overall efficiency (η)	6.0%
Mass without fuel or tank (m_{eng})	14 kg (30 lb)

listed in Table 3. The Fuji-based HEPU was evaluated on a test stand, but not fully constructed due to its high noise level.

3.5. ZDZ80-based HEPU

A HEPU system with integrated noise-deadening measures was realized with a ZDZ80 two-stroke engine. Figure 8 shows a CAD image of the system. The system specifications are listed in Table 4. See Section 4 on the ZDZ80 HEPU for a detailed description of the design of this power unit.

4. DETAILED DESIGN OF THE ZDZ80-BASED HEPU

We now describe in detail the design of the ZDZ80-based HEPU — the most sophisticated of the HEPU units.

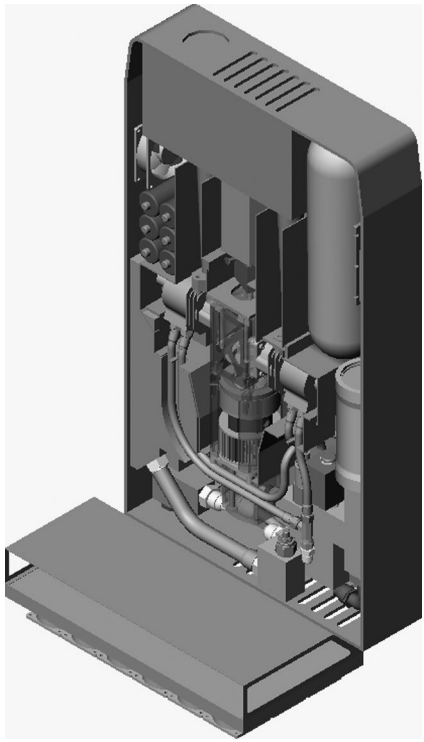

Figure 8. ZDZ80 HEPU.

Table 4.
ZDZ 80 HEPU specifications

Description	Fourth-generation HEPU
Engine	ZDZ-80 2-stroke, liquid-cooled, direct-drive
Hydraulic power	2.3 kW (20 LPM @ 6.9 MPa) 3.0 HP (5.2 GPM @ 1000 p.s.i.)
Electrical power	220 W (Kollmorgen RBE series, three-phase brushless motor/alternator)
Transmission	In-line direct drive of pump and alternator
Hydraulic pump	Haldex W300 gear pump
Pressure and voltage control	Solenoid hydraulic bypass valve, computer-controlled engine speed
Overall efficiency (η)	8.1%
Mass without fuel or tank (m_{eng})	27 kg (59 lb)

4.1. HEPU specifications

The design requirements for a mobile fieldable robotic system are functions of the robot size, its maneuvering speed and its payload capability. The design of the hybrid power unit described here was motivated by the requirements of the BLEEX project [12–14]. After designing several HEPUs, we have come to realize

that mobile robotic systems with similar weight and size to BLEEX will require power sources with the same characteristics which differ only nominally. The main feature of BLEEX and many other field robotic systems that effects the design of their power units is the load-carrying capability in the field. While many walking systems [16, 17] are designed to carry only their own weight, BLEEX was designed to carry external loads.

While high-pressure hydraulics often leads to less power loss, we chose 6.9 MPa (1000 p.s.i.) as the system pressure. This leads to more reasonable hydraulic components for mobile systems that need to work in the field and perhaps in proximity of humans. We recommend higher working pressure (e.g., 20.7 MPa or 3000 p.s.i.) if safe and appropriate hydraulic delivery components can be incorporated in the system. The hydraulic flow requirements are usually calculated using the speed characteristics of the robot. High-speed movements lead to large hydraulic flow requirements. In the case of the BLEEX project, the walking speed from clinical gait analysis (CGA) data [12] resulted in 20 LPM (5.2 GPM) of hydraulic flow. Our experience in building various exoskeleton systems suggest that one requires approximately 220 W of electric power for on-board robot computers and sensors in addition to the power unit sensors and controller.

4.2. Overall HEPU architecture

The HEPU is designed to provide electric and hydraulic power. It uses a compact two-stroke opposed twin cylinder IC engine capable of all-angle operation. Figures 9 and 10 show how the engine (1) drives a single shaft (2) to power an alternator (3) for electric power generation, a cooling fan (4) for air circulation and a gear pump (5) for hydraulic power generation. This single shaft design elegantly avoids noisy and heavy belt drive mechanisms common in systems comprising many rotating shafts. A hydraulic solenoid valve (7) regulates the hydraulic fluid pressure by directing the hydraulic flow from the gear pump to either an accumulator (10) or to the hydraulic reservoir (13). The accumulator consists of an aluminum cylinder in which a free piston separates the hydraulic fluid from the pressurized nitrogen gas. A carbon fiber tank (11) is attached to the gas side of the accumulator as reservoir for the nitrogen gas. In general, the larger the volume of this gas reservoir is, the smaller the pressure fluctuation will be in the presence of hydraulic flow fluctuations. A pressure transducer (9) measures the pressure of the hydraulic fluid for the controller. A manifold (6) is designed to house both the solenoid valve (7) and filter (8). A novel liquid cooling scheme utilizes the returning hydraulic fluid itself to cool the engine. The hydraulic fluid from the robot actuators is divided into two paths. Approximately 38% of the hydraulic fluid is diverted to cool the engine cylinders. A heat exchanger (12) removes the heat from this hydraulic fluid before it reaches the hydraulic reservoir (13) and is mixed with the remaining 62% of the fluid.

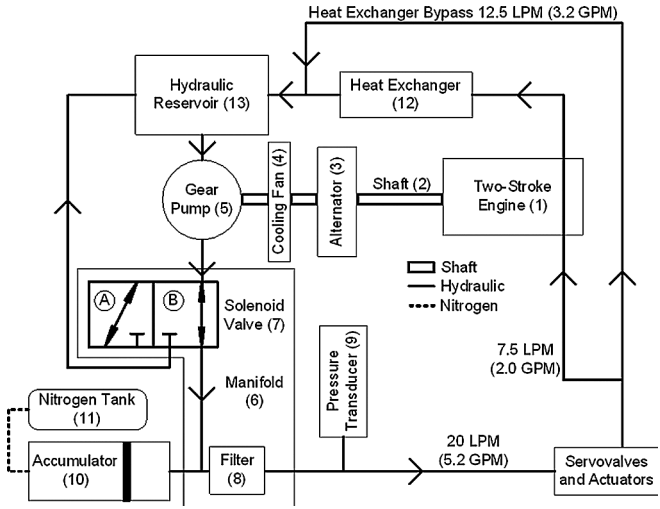

Figure 9. HEPU schematic layout. Components labeled with numbers in parentheses also correspond to Fig. 10.

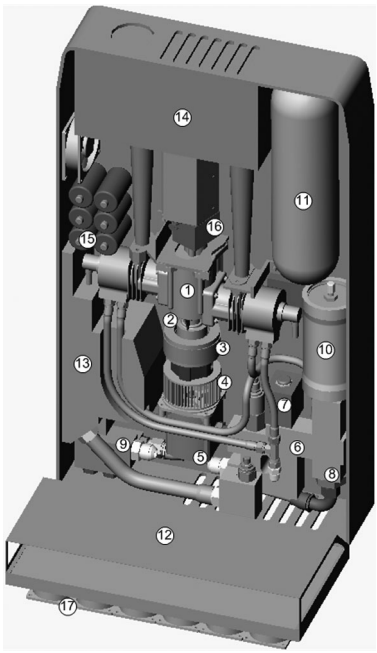

Figure 10. HEPU physical layout. Engine (1); shaft (2, not visible); alternator (3); cooling fan (4); gear pump (5); manifold (6); solenoid valve (7); filter (8, not visible); pressure transducer (9, not visible); accumulator (10); nitrogen tank (11); heat exchanger (12); hydraulic reservoir (13); muffler (14); batteries (15); carburetor and throttle (16); heat exchanger fans (17). Internal baffling around engine is not shown for clarity.

4.3. Mechanical power production

The two-stroke opposed twin cylinder IC engine (model 80 B2 RV; ZDZ Model Motor) capable of producing 6 kW (8.1 hp) of shaft power at 8200 r.p.m. is used as the prime mover of this power unit. This engine has an 80 cm^3 displacement and weighs only 2 kg (4.4 lb). Since the gear pump was limited to turn at maximum speed of 6300 r.p.m. and since we intended not to utilize any transmission speed reducer in this power unit, we were forced to drive the engine at speeds lower than the maximum-power speed of the engine. The engine can produce approximately 3.06 kW (4.0 hp) at 6300 r.p.m. which is greater than the required power (2.5 kW or 3.4 hp). In general, using a larger engine at lower speeds results in less noise than using a smaller engine at higher speeds. The engine is controlled with a servo motor mounted to its throttle.

The engine directly drives an alternator, a cooling fan and a gear pump. The pump (model WP03-B1B-032L-20MA12; Haldex) has a 3.2 cm^3 displacement volume per revolution and therefore in theory it can transfer 20.2 LPM (5.3 GPM) of flow at its maximum speed of 6300 r.p.m.

4.4. Control architecture

A unique control scheme was needed to maintain constant operating pressure with a fixed displacement pump running at a constant speed. An accumulator at the outlet of the pump supplies the fluid to the actuators and functions like a capacitor to compensate for transient peak flows. The hydraulic pressure is read by the pressure sensor. The computer controls the solenoid valve to maintain the pressure. When the pressure reaches the desired value (6.9 MPa in this case), the computer diverts the hydraulic flow to the reservoir by moving the valve to position A as shown in Fig. 9. To prevent pressure drop in the accumulator when the hydraulic fluid in the accumulator is consumed by the servovalves and the actuators, the computer diverts the flow to the accumulator by moving the valve to position B. The modulation of this valve based on the measured pressure allows the system to output hydraulic power at near constant pressure. The operating pressure in the accumulator is maintained in a band of 6.9 ± 0.2 MPa (1000 ± 30 p.s.i.).

When the solenoid valve diverts the hydraulic fluid to the reservoir, the engine speed increases rapidly. The opposite is also true: when the valve diverts the hydraulic fluid to the accumulator, the engine speed decreases rapidly and the engine might even stall. The variation of engine speed causes exhaust sound with varying frequencies that is undesirable for optimal noise reduction. Furthermore, the engine speed variation leads to a large voltage variation. Additionally the high engine speeds might damage the pump. For the above reasons, it is desirable to control the engine speed to a constant value. It was decided to maintain the speed at 6300 r.p.m. (maximum allowable pump speed). In summary, an on-board computer uses a pressure sensor and a Hall effect sensor to regulate the pressure (at 1000 p.s.i.)

and engine speed (at 6300 r.p.m.) by modulating a hydraulic solenoid valve and an engine throttle.

4.5. Cooling

Since the engine was designed for high-performance model aircraft, it requires a large amount of air for cooling its cylinders (air is generously available when the engine is installed on aircraft models). For the application of field robotics, it is necessary to package the engine tightly in a sound-deadening shield; therefore, liquid cooling was required. A novel liquid cooling scheme was devised that uses the hydraulic fluid itself to cool the engine. The engine cylinder heads were modified to allow hydraulic fluid to pass through them and absorb heat (Fig. 11). This makes the addition of a water-based cooling system unnecessary and results in a simplified system with fewer components. Using the hydraulic fluid as the cooling medium increases the load on the heat exchanger since the heat from the engine must be removed to prevent the hydraulic fluid from exceeding the operating temperature of any hydraulic components. The maximum temperature allowable was determined by the pump which had the lowest temperature tolerance of any component in the system (the gear pump required hydraulic fluid temperature cooler than 65°C or 149°F).

The fluid returning from the actuators is split into two separate paths, as shown in Fig. 12. Approximately 62% of the hydraulic fluid returns directly to the reservoir. The remaining 38% passes first through the cylinder heads where excess heat is extracted from the engine, then through a heat exchanger where the heat in the fluid is dissipated and, finally, returns to the reservoir. As shown in Fig. 12, the heat exchanger must remove the heat generated from the dissipative effect of the servovalves on the actuators in addition to the heat generated in the engine cylinder heads. Increasing fluid volume in the reservoir increases convective heat transfer (cooling) to ambient air and allows longer operation times. This is a typical solution

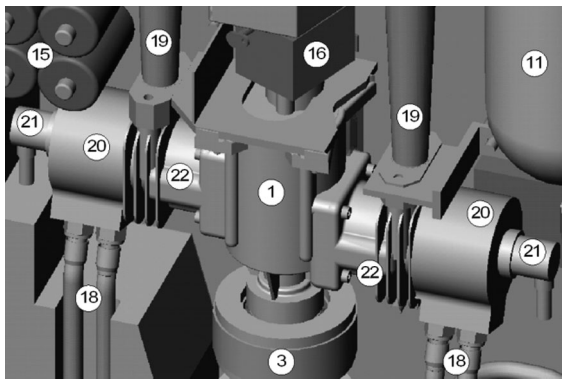

Figure 11. Detail of the engine depicting the cooling jackets on the cylinders. Engine (1); alternator (3); nitrogen tank (11); batteries (15); carburetor and throttle (16); hydraulic lines (18); exhaust pipe (19); cooling jacket (20); spark plug (21); cylinder head (22).

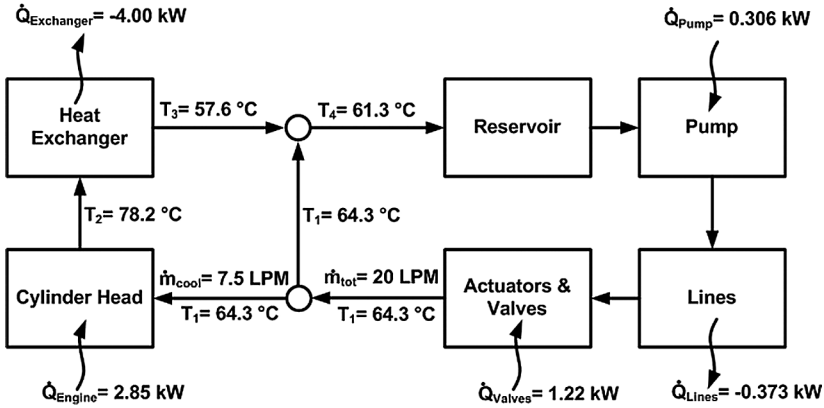

Figure 12. Cooling system schematic of the HEPU.

in industrial hydraulics, but is not feasible in this application where a large reservoir is undesirable. Therefore, careful sizing of the heat exchanger was critical to ensure adequate cooling at a minimum weight.

A thermal model was created (using measured data from the test stand whenever possible) to estimate the behavior of the hydraulic system and evaluate the hydraulic fluid temperature at the most sensitive component, the pump. Data was taken from an experimental run with the engine producing 3.06 kW of shaft power. A duty cycle of 50% was used to simulate our operating conditions (i.e., 1.53 kW continuous shaft power). The reservoir was modeled as a perfect mixer with zero heat transfer, to ambient. The pump exhibited a minimum of 80% efficiency (shaft power to fluid power); hence, 20% of the engine shaft power ($3.06\ \text{kW} \times 0.50 \times 0.20 = 0.306\ \text{kW}$ or 0.41 hp) was converted to heat into the hydraulic fluid. The heat transfer to ambient air in the hydraulic lines was estimated at -0.373 kW (-0.50 hp). The actuators and servovalves were assumed to convert all the hydraulic power flowing through them to heat into the hydraulic fluid ($3.06\ \text{kW} \times 0.50 \times 0.80 = 1.22\ \text{kW}$ or 1.64 hp). The sum of the heat transfer rates from the reservoir, pump, lines and valves is $\dot{Q}_{\text{Other}} = (1.22 + 0.306 - 0.373) = 1.15$ kW (1.54 hp). The heat transfer rate from the engine cylinders, $\dot{Q}_{\text{Engine}}$, was measured at 2.85 kW (3.82 hp). The performance of the heat exchanger is characterized by a thermal parameter K_{th}, which is the heat transfer rate at a given flow rate of fluid divided by the initial temperature difference between the hot fluid entering the heat exchanger and the environment at T_{ambient}:

$$\dot{Q}_{\text{Exchanger}} = -K_{\text{th}}(T_2 - T_{\text{ambient}}). \tag{9}$$

The temperature T_4 in Fig. 12 is equal to the pump inlet temperature since there is no heat transfer in the reservoir. At steady state the heat transfer from each component can be expressed by the following equations.

$$\dot{Q}_{\text{Other}} = \dot{m}_{\text{total}} c_{\text{P}}(T_1 - T_4), \tag{10}$$

$$\dot{Q}_{\text{Engine}} = \dot{m}_{\text{cool}} c_{\text{P}}(T_2 - T_1), \tag{11}$$

$$\dot{Q}_{\text{Exchanger}} = \dot{m}_{\text{cool}} c_{\text{P}} (T_3 - T_2), \tag{12}$$

where $\dot{m}_{\text{total}}$ is the total hydraulic mass flow rate, $\dot{m}_{\text{cool}}$ is the cooling flow rate and c_{P} is the specific heat of the fluid. Since at steady state:

$$\dot{Q}_{\text{Exchanger}} + \dot{Q}_{\text{Engine}} + \dot{Q}_{\text{Others}} = 0. \tag{13}$$

Equations (9)–(13) can be solved explicitly for the steady-state pump inlet temperature, T_4:

$$T_4 = T_{\text{ambient}} - \frac{\dot{Q}_{\text{Exchanger}}}{K_{\text{th}}} - \frac{\dot{Q}_{\text{Engine}}}{\dot{m}_{\text{cool}} c_{\text{P}}} - \frac{\dot{Q}_{\text{Other}}}{\dot{m}_{\text{total}} c_{\text{P}}}. \tag{14}$$

Various heat exchanger specifications were inserted in (14) to estimate the steady-state hydraulic fluid temperature and evaluate the performance of a given heat exchanger. At steady state the selected heat exchanger removes 4.00 kW and the calculated pump inlet temperature is 61°C (141°F), under the maximum allowable pump temperature, 65°C.

4.6. Electrical power generation

The HEPU generates electrical power for the sensors, cooling fans and control computer. The electrical power generation and regulation design is depicted in Fig. 13. The total electrical system power budget is 220 W, with 100 W for cooling fans, and 65 W for the control computer and sensors. The remaining 55 W are expected to be consumed in losses and other peripheral components. A three-phase, 12-pole frameless, brushless DC motor (model RBE-1812; Kollmorgen) is used as an electric power generator (3 in Fig. 10). The three phases were converted to single-phase, 240 V DC by a bridge rectifier (the back-EMF constant of the motor is 26.9 V/k.r.p.m. so that at the operational speed of 6300 r.p.m. the rectified voltage is 240 V DC). Two DC–DC converters are used to create two 15 V DC bus voltages to be used for two sets of components. One 15 V DC line is used to power the electrically noisy components such as solenoid valves, cooling fans and the ignition for the engine. The second 15 V DC line is used to charge a set of batteries, and power the control computer, HEPU controller and throttle servo. The external power (shown in Fig. 13) is used to power the system when the engine is off. The battery shown in Fig. 13 powers the control computer, HEPU controller, throttle servo and sensors for a short time in case the engine shuts down. This gives the operator ample time to connect external power to the system. The HEPU controller measures and regulates two important variables: engine speed and hydraulic pressure. While regulation of the hydraulic pressure is important for the robot control, regulation of the engine speed manifests to a constant output voltage and constant engine noise frequency. A constant engine noise frequency is important in the design of an optimal muffler. The engine speed is measured by counting the pulses from a Hall effect sensor on the alternator. The HEPU controller outputs are the solenoid valve and servo. While the solenoid valve regulates the pressure, the servo ensures

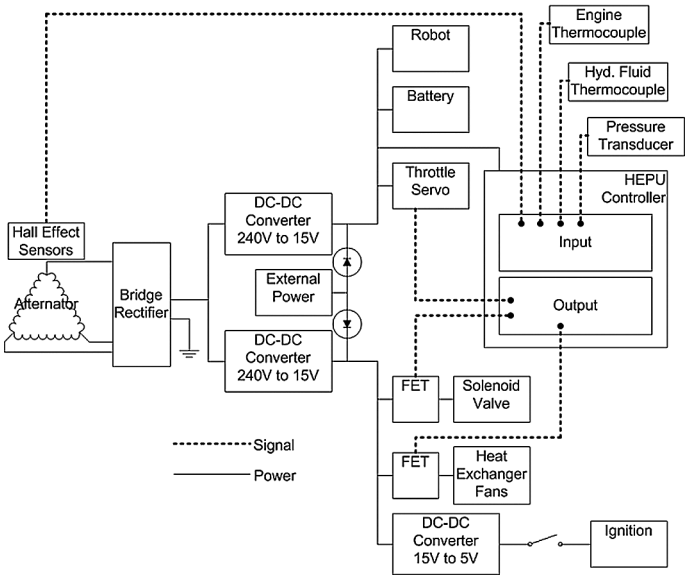

Figure 13. Electrical schematic.

constant speed (6300 r.p.m.). The HEPU also measures engine and hydraulic fluid temperature and controls the heat exchanger fans (17 in Fig. 10).

4.7. HEPU layout

Any robotic power source must be packaged so that it leaves a maximum of useable space for the robot and its payload. It is simplest to package the power source by layering components around the engine, but this tends to create a roughly cubic shape that must be integrated into the robotic system. The HEPU design focused on creating a power source that was as thin as possible in one dimension to make integration simple. Such a design may be attached to a robotic system on any available side or in any available space without impeding its functionality. Since the heat exchanger for cooling must exhaust freely to the atmosphere, it is left as a separate attachment to be placed as convenient. In Fig. 10 it is shown on the bottom of the power source as a shelf so that payload could be placed above the heat exchanger.

Reducing the thickness of the power source drove many of the design decisions. The two-stroke engine has a carburetor mounted parallel to the crankshaft and can be configured so that the exhaust ports are also parallel to the crankshaft, which allows it to fit in an extremely thin package. Similarly, the fuel was stored in the hollow back panel of the device rather than a separate fuel tank. Even the muffler was custom designed to fit exactly into the power source. The result was a 10-cm (4-inch) thick power source design that could be integrated into many robotic systems.

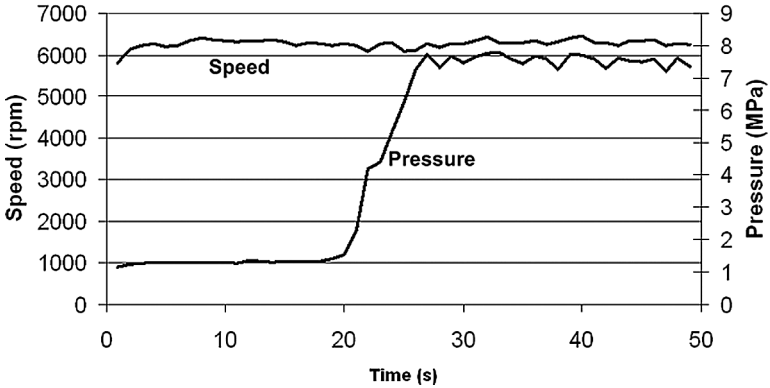

Figure 14. Automatic throttle control on the test stand.

4.8. Noise abatement

At the outset of the HEPU design, a 78 dBA noise specification was set (measured at a distance of 1.5 m or 5 ft from the HEPU at full power); 75 dBA is approximately the noise level of a commercially available 2-kW generator, which uses a quieter four-stroke engine. Reaching such a low level of noise with a two-stroke engine, notorious for high noise levels, was probably unrealistic. Two strategies were used to reduce the noise to tolerable levels. First, the engine was set to run at a constant r.p.m. so that the muffler could be optimized to constant frequencies. Second, direct paths to the engine were eliminated through the use of liquid cooling and baffles around the engine. Two nested sheet metal containment shells were constructed using welded 1.6-mm (0.062-in) thick aluminum and placed over the engine. The containment shells were sprayed on both sides with 2–3 mm of viscoelastic damper material. The inside of the containment shells was further lined with 10-mm-thick open cell polyimide foam. An intake muffler was constructed using an aluminum box filled with polyester reticulated foam. The muffler was used with its output pipe exhausting outside of both containment shells. The best noise level obtained when measured outdoors was 87 dBA, significantly above the desired noise level of 78 dBA. The muffler is responsible for the greatest sound reduction; the sound shield was marginally effective.

4.9. Performance evaluation

An instrumented test stand was built with all the components of the HEPU design except the electrical system and pressure regulation, which are similar to those installed on older BLEEX power units. Figure 14 shows an experiment where the system pressure is changed from 1.4 to 7.5 MPa while the controller maintains a constant speed. Testing also confirmed that the HEPU approximately met the flow requirements with 19.4 LPM (5.1 GPM) of flow at a pressure of 7.4 MPa (1073 p.s.i.) resulting in 2.4 kW (3.2 hp) of hydraulic power, as shown in the steady-state run in Fig. 15.

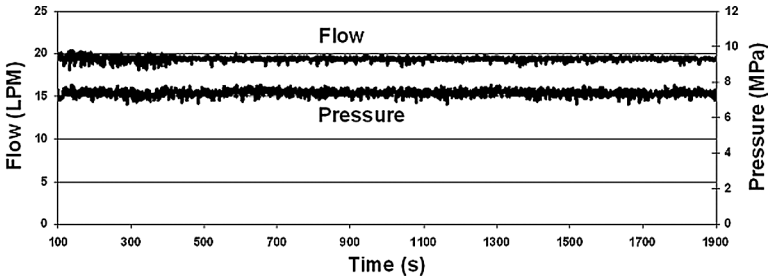

Figure 15. The power source is able to produce 19.4 LPM at 7.4 MPa. No accumulator was installed on the test stand to compensate for transient effects.

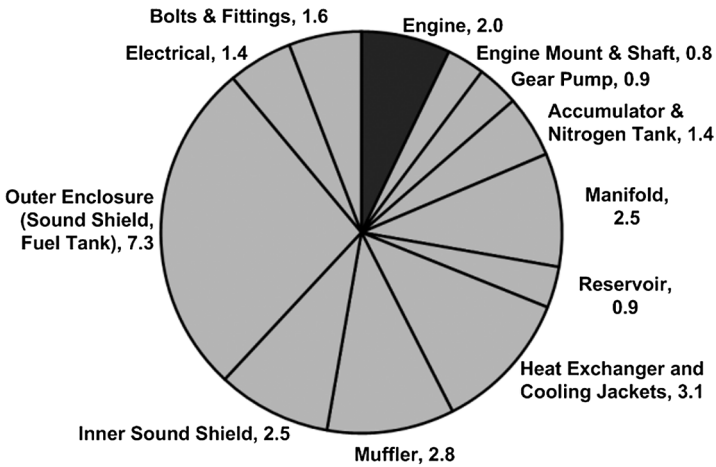

Figure 16. Mass budget (in kg) (27 kg total).

Figure 16 shows the mass budget for the power unit. The power unit reached an approximate dry mass of 27 kg of which the engine itself contributes only 2 kg (about 7%). Therefore, in pursuing a lighter design, one must reduce the mass of other components instead of focusing solely on the engine.

5. CONCLUSION

The design and testing of the HEPUs shows that gasoline-fueled hydraulic power units are viable options for powering mobile robotic devices. We have found that long mission times with high electrical and mechanical power demands can be met only by taking advantage of the high specific energy of gasoline. Furthermore, we recommend the use of Ragone plots for determining the best design of a power unit so that the power system mass is minimized for a given operation time. Based on our experience with the HEPUs, we have arrived at the ZDZ80-based HEPU design, which successfully produces constant-pressure hydraulic power (2.3 kW) and constant-voltage electrical power (220 W) for a mobile robotic system.

Acknowledgements

This work is partially funded by DARPA grant DAAD19-01-1-0509.

REFERENCES

1. Y. Sakagami, R. Watanabe, C. Aoyama, S. Matsunaga, N. Higaki and K. Fujimura, The intelligent ASIMO: system overview and integration, in: *Proc. IEEE/RSJ Int. Conf. on Intelligent Robots and Systems*, Lausanne, pp. 2478–2483 (2002).
2. High-energy lithium-ion cell, VL 45 E cell, *Document 54032-2-0603*, Communication Department, SAFT, Bagnolet (2003).
3. J. W. Raade, T. G. McGee and H. Kazerooni, Design, construction, and experimental evaluation of a monopropellant powered free piston hydraulic pump, in: *Proc. ASME Int. Mechanical Engineering Congr. and Exp.*, Washington, DC, pp. 651–658 (2003).
4. T. G. McGee, J. W. Raade and H. Kazerooni, Monopropellant-driven free piston hydraulic pump for mobile robotic systems, *ASME J. Dyn. Syst. Meas. Control* **126**, 75–81 (2004).
5. E. J. Barth, M. A. Gogola, J. A. Wehrmeyer and M. Goldfarb, The design and modeling of liquid-propellant-powered actuator for energetically autonomous robots, in: *Proc. ASME Int. Mechanical Engineering Congr. and Exp.*, New Orleans, LA, pp. 917–923 (2002).
6. M. Gogola, E. J. Barth and M. Goldfarb, Monopropellant powered actuators for use in autonomous human scale robotics, in: *Proc. IEEE Int. Conf. on Robotics and Automation*, Washington, DC, pp. 2357–2362 (2002).
7. P. Weiss, Dances with robots, *Sci. News* **159**, 407–408 (2001).
8. E. Colin, D. Polome, V. Piedfort and Y. Baudoin, AMRU 3: a teleoperated six-legged electro-hydraulic robot, in: *Proc. SPIE*, Vol. 2352, pp. 192–203 (1995).
9. K. Amundson, J. Raade, N. Harding and H. Kazerooni, Hybrid hydraulic–electric power unit for field and service robots, in: *Proc. IEEE Intelligent Robots and Systems*, Edmonton, pp. 3453–3458 (2005).
10. J. W. Raade, K. Amundson and H. Kazerooni, Development of hydraulic–electric power units for mobile robotics, in: *Proc. ASME Int. Mechanical Engineering Congr. and Exp. Fluid Power Systems Technology Division*, Orlando, FL, pp. 27–34 (2005).
11. J. W. Raade and H. Kazerooni, Analysis and design of a novel hydraulic power source for mobile robots, *IEEE Trans. Automat. Sci. Eng.* **2**, 226–232 (2005).
12. A. Chu, H. Kazerooni and A. Zoss, On the biomimetic design of the Berkeley Lower Extremity Exoskeleton (BLEEX), in: *Proc. IEEE Int. Conf. on Robotics and Automation*, Barcelona, pp. 4345–4352 (2005).
13. H. Kazerooni, L. Huang, J. L. Racine and R. Steger, On the control of Berkeley Lower Extremity Exoskeleton (BLEEX), in: *Proc. IEEE Int. Conf. on Robotics and Automation*, Barcelona, pp. 4353–4360 (2005).
14. A. Zoss and H. Kazerooni, On the mechanical design of the Berkeley Lower Extremity Exoskeleton (BLEEX), in: *Proc. IEEE Intelligent Robots and Systems*, Edmonton, pp. 4345–4352 (2005).
15. C. Grimmer, Mechanical design and testing of an exoskeleton hydraulic power unit, MSc Thesis, University of California, Berkeley, CA (2005).
16. H. Kawamoto and Y. Sankai, Power assist system HAL-3 for gait disorder person, in: *Proc. 8th Int. Conf. on Computers Helping People with Special Needs*, Berlin, pp. 196–203 (2002).
17. M. Vukobratovic, B. Borovac, D. Surdilovic and D. Stokic, Humanoid robots, in: *Mechanical Systems Design Handbook*, O. Nwokah and Y. Hurmuzlu (Eds), pp. 707–726. CRC Press, Boca Raton, FL (2002).

ABOUT THE AUTHORS

Kurt Amundson received the B.S. degree from Washington University in St. Louis, and the M.S. degree from the University of California, Berkeley. He is currently a Ph.D. student in the Robotics and Human Engineering Laboratory at the University of California, Berkeley. Mr. Amundson's research interests include control of robotic and mechatronics systems and mobile robotic power systems.

Justin W. Raade received the B.S. degree from the Massachusetts Institute of Technology in Cambridge, Massachusetts and the M.S. and Ph.D. degrees from the University of California, Berkeley, all in mechanical engineering. He is currently a researcher in the Robotics and Human Engineering Laboratory at the University of California, Berkeley. Dr. Raade's research includes robotics and mechatronics, novel power sources, and portable fuel cells.

Nathan Harding received the B.S. in mechanical engineering and economics from Carnegie Mellon University in Pittsburgh and the M.S. in mechanical engineering from the University of California, Berkeley. Mr. Harding has worked as a consultant to the Robotics and Human Engineering Laboratory, and has served as Mechanical Engineering Manager at Berkeley Process Control.

H. Kazerooni received the M.S. and Ph.D. degrees in mechanical engineering from the Massachusetts Institute of Technology, Cambridge, Massachusetts, in 1982 and 1984, respectively. He is currently a Professor in the Mechanical Engineering Department at the University of California, Berkeley and Director of the Robotics and Human Engineering Laboratory.